crystals

MDPI

Article

Structural and In Situ X-ray Diffraction Study of Hydrogenation of $Ca_xMg_{1-x}Ni_2$ ($0 \leq x \leq 1$)

Zia Ur Rehman [1], Mohsan Nawaz [1,*], Hameed Ullah [2], Pervaiz Ahmad [3], Mayeen Uddin Khandaker [4], Abubakr M. Idris [5,6], Sirajul Haq [7,*] and Abdelmoneim Sulieman [8]

1 Department of Chemistry, Hazara University Mansehra, Mansehra 21300, Pakistan; ziamwt1@gmail.com
2 Department of Chemistry, Islamia College University, Peshawar 25120, Pakistan; hameedullah@icp.edu.pk
3 Department of Physics, University of Azad Jammu and Kashmir, Muzaffarabad 13100, Pakistan; pervaiz_pas@yahoo.com
4 Centre for Applied Physics and Radiation Technologies, School of Engineering and Technology, Sunway University, Bandar Sunway 47500, Malaysia; mayeenk@sunway.edu.my
5 Department of Chemistry, College of Science, King Khalid University, Abha 61421, Saudi Arabia; abubakridris@hotmail.com
6 Research Center for Advanced Materials Science (RCAMS), King Khalid University, Abha 61421, Saudi Arabia
7 Department of Chemistry, University of Azad Jammu and Kashmir, Muzaffarabad 13100, Pakistan
8 Department of Radiology and Medical Imaging, College of Applied Medical Sciences, Prince Sattam Bin Abdulaziz University, P.O. Box 173, Al-Kharj 11942, Saudi Arabia; a.sulieman@psau.edu.sa
* Correspondence: mohsannawaz@hotmail.com (M.N.); cii_raj@yahoo.com (S.H.)

Abstract: In the quasi-binary system $CaNi_2$-$MgNi_2$ solid-solutions $Ca_xMg_{1-x}Ni_2$ ($0 \leq x \leq 1$) were prepared from the elements. They crystallize in the hexagonal Laves phase type ($MgNi_2$, *C*36) for $x \leq 0.33$ ($P6_3/mmc$, a = 482.51(7) pm, c = 1582.1(3) pm for x = 0, a = 482.59(3), c = 1583.1(1) for x = 0.33) and in the cubic Laves phase type ($MgCu_2$, *C*15) for $0.33 < x$ ($Fd\bar{3}m$, a = 697.12(3) pm for x = 0.5, a = 705.11(2) pm for x = 0.67, a = 724.80(2) pm for x = 1). After hydrogenation in an autoclave the X-ray diffraction patterns changed completely. Reflections assigned to $CaNiH_3$, and Ni and Rietveld refinement confirmed this. The hydrogenation properties of $Ca_xMg_{1-x}Ni_2$ ($0 \leq x \leq 1$) compounds were also studied in situ by X-ray powder diffraction. In situ X-ray powder diffraction of $Ca_xMg_{1-x}Ni_2$ ($0 \leq x \leq 1$) compounds under 0.3 MPa hydrogen gas flow (15 sccm), data collected on a Rigaku SmartLab diffractometer in an Anton Paar XRK 900 Reactor Chamber using Cu-Kα1 radiation. Scanning electron microscopy and EDX spectroscopy confirmed the entitled materials and elemental composition, respectively. From the Transmission electron microscopy and Selected area electron diffraction concluded that the $Ca_xMg_{1-x}Ni_2$ ($0 \leq x \leq 1$) compounds were crystalline.

Keywords: hydrogen storage; metal hydrides; X-ray diffraction; in situ techniques; microscopy

check for updates

Citation: Rehman, Z.U.; Nawaz, M.; Ullah, H.; Ahmad, P.; Khandaker, M.U.; Idris, A.M.; Haq, S.; Sulieman, A. Structural and In Situ X-ray Diffraction Study of Hydrogenation of $Ca_xMg_{1-x}Ni_2$ ($0 \leq x \leq 1$). *Crystals* **2022**, *12*, 47. https://doi.org/10.3390/cryst12010047

Academic Editors: Jacek Krawczyk, Wlodzimierz Bogdanowicz and Bo Liu

Received: 23 November 2021
Accepted: 26 December 2021
Published: 30 December 2021

Publisher's Note: MDPI stays neutral with regard to jurisdictional claims in published maps and institutional affiliations.

Copyright: © 2021 by the authors. Licensee MDPI, Basel, Switzerland. This article is an open access article distributed under the terms and conditions of the Creative Commons Attribution (CC BY) license (https://creativecommons.org/licenses/by/4.0/).

1. Introduction

The growing awareness of environmental protection and increasing demands for energy force us to find a new complementary solution. To replace traditional fossil fuels, hydrogen is receiving interest as a clean energy. Finding a new way to store hydrogen is the main problem in using hydrogen as a fuel in the future. To store hydrogen in the solid phase is the most promising solution because of the reversibility of the process, for safety reasons and, above all, its high capacity [1–8]. There are many materials that can be used as a medium for hydrogen storage. For hydrogen storage AB, AB_2, A_2B and AB_5 intermetallic phase-based alloys are the one basic group of materials [9]. In term of hydrogen storage, magnesium hydride is the mostly studied materials because of reversible absorption and desorption, high gravimetric density and relatively low cost [10]. The problem is that the high thermodynamics stability and slow kinetics of its absorption and desorption reactions complicate its uses. There are a number of publications regarding the possibility of improving these properties, mainly by doping with transition group elements

or other chemical compounds and the formation of ternary metal hydrides [11–14]. Low-cost hydrogen storage materials include calcium-nickel and magnesium-calcium-nickel alloys. Many new hydrogen-absorbing materials have been developed to increase hydrogen storage capacity. Low-density Ca-Ni alloys are also good for hydrogen storage applications; for example, the $CaNi_5$ alloy absorbed 1.9 percent hydrogen [15]. With a $PuNi_3$ structure, the $Ca_{0.4}Mg_{0.6}Ni_3$ alloy has a hydrogen capacity of 1.56 percent at room temperature [16–18]. The $MgCu_2$ type (C15), $MgZn_2$ type (C14), and $MgNi_2$ type are the three main types of Laves phases (C36). For some subgroups, such as AM_2 and AM_3, both elements from the main groups, but occasionally M from the transition metal, valence electron concentration and size ratio are known [19–21]. Many Laves phases take up hydrogen reversibly at moderate pressure and temperature, making them a common example of hydrogen storage materials [22–25]. A statistical rule AMm + nH_2 = $AMmH_2n$ was developed for the thermodynamic hydrogen uptake of an intermetallic phase [26]. $CaNi_2$ and $MgNi_2$ have cubic and hexagonal crystal structure, respectively. $Ca_xMg_{1-x}Ni_2$ (x = 0.5, 0.67) also has cubic and C15 ($MgCu_2$)-type Laves phase structure while $Ca_xMg_{1-x}Ni_2$ (x = 0.33) has hexagonal and C36 ($MgNi_2$)-type Laves phase structure (Figure 1).

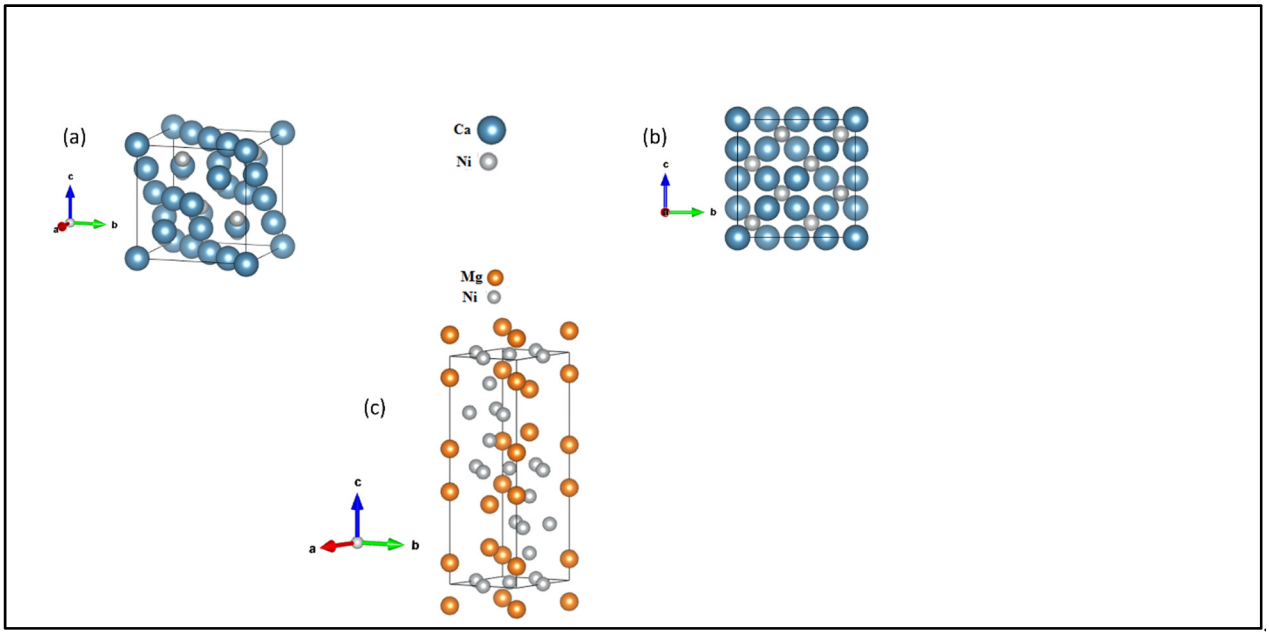

Figure 1. Crystal structures of (**a**,**b**) $CaNi_2$ (**c**) $MgNi_2$.

Oesterreicher et al. [27] investigated the hydrogen storage properties and crystal structure of the $Ca_{1-x}Mg_xNi_2$ alloy first, and Terashita et al. [28] investigated it further. $CaNi_2$ belongs to the C15 Laves phase, whereas $MgNi_2$ belongs to the C36 Laves phase. Terashita claims that the single C15 Laves phase exists in the $CaNi_2$ and $Ca_{0.32}Mg_{0.68}Ni_2$ composition ranges and was absorbed hydrogen 1.4 percent at 313 K. Basic structural units for the Hauke (AB5) and Laves (AB2) phases have been identified. $CaMg_2$($MgZn_2$ type), Mg_2Ni, and C36 $MgNi_2$ Laves phases are known complementary phases in the Ca-Ni and Mg-Ni binary systems. The Mg position at A or B sites in the Laves phases results different polytypes formation in the system. From the structural point of view this was widely studied by Komura group in 1980s [29]. Shin-ichi Orimo et al. have studied the nano-structured and amorphous-structured hydriding properties in the binary Mg-based system [30,31]. Akiba and Tsushio have thoroughly investigated the $Mg(Ni_{1.9}M_{0.1})$ (M = Cr, Mn, Fe) with the AB-type Laves phases structure hydriding properties in the ternary system [32,33]. Oesterreicher et al. have reported the $(Mg_xR_{1-x})Ni_2$ (x = 0–1.0, R = Ca, La) hydriding properties [34]. Terashita et al. studied the $Mg_{1-x}Ca_xNi_2$ hydriding properties [28] and Kohno et al., have studied the Mg-La-Ni hydriding properties [35].

The objective of this study to obtain more data for the hydrogenation of $CaNi_2$, $MgNi_2$ and $Ca_xMg_{1-x}Ni_2$ compounds. The hydrogenation properties of the above-mentioned compounds were analyzed in situ by X-ray diffraction (XRD). In the present article we also synthesized and characterized the binary alloys of $CaNi_2$, $MgNi_2$ and ternary alloy of $Ca_xMg_{1-x}Ni_2$ (x = 0.5, x = 0.67, x = 0.33). $Ca_xMg_{1-x}Ni_2$ which are pseudo binary alloy based on $CaNi_2$ (C15 Laves phase) and $MgNi_2$ (C36 Laves phase).

2. Materials and Methods

2.1. Materials

The $Ca_xMg_{1-x}Ni_2$ ($0 \leq x \leq 1$) compounds were prepared from the elements Mg powder (99.9%, −325 mesh, Alfa Aesar, Karlsruhe, Germany) Ca granules redistilled (99.9%, metal basis 1 cm (0.4 in) Alfa Aesar, Karlsruhe, Germany) and Ni powder (99.9%, −100 mesh, Aldrich, Seelze, Germany).

2.2. Synthesis

It is rather difficult to get the accurate stoichiometry in the $Ca_xMg_{1-x}Ni_2$ system because synthesis is hindered due to the low boiling point of calcium 1873 K (1600 °C) which is close to the nickel melting point 1728 K (1455 °C). Therefore, during melting of both elements together leads to losses of calcium by evaporation. Mg addition also leads to the same problems. Different Ca-Mg-Ni samples were prepared by sealing the starting materials into Ta tubes under the argon atmosphere inside the gloves box finally completely sealed by arc melting [36]. Based on stoichiometric amounts of starting materials, an extra 2 wt.% of Ca and 6 wt.% of Mg were therefore added to compensate for the losses of Ca and Mg during reaction. All mixtures were sealed in Ta tubes under argon atmosphere by arc melting and heated from room temperature to T = 920 °C over 100 °C/h, held for 2 h, cooled to T = 800 °C within 1 h and 12 min, then held for 6 h and finally cooled to room temperature under vacuum 10^{-3} mbar.

In an argon-filled gloves box with oxygen and water content below 1 ppm, all alloys were mechanically crushed into powders. Laboratory XRPD data were collected using either a Huber G670 diffractometer with Mo-K1 radiation (flat transmission sample with Lithilen® grease between two Kapton® foils) or a Rigaku D/Max 2500VL/PC diffractometer (provided by Rigaku Corporation, Tokyo, Japan) with Cu Ka radiation at 50 kV and 150 mA.

2.3. Hydrogenation

For hydrogenation the powdered intermetallic binary and ternary alloys i.e., $Ca_xMg_{1-x}Ni_2$ (x = 1, x = 0.67, x = 0.33 and x = 0) (100 mg) each sample was placed in a hydrogen resistant stainless steel (nickel-chromium stainless steel 1.4571) crucible in autoclave made from the same alloy, charged with hydrogen (≥99.9%, Air Liquide, Paris, France) and heated in a vertical tube furnace. The hydrogen pressure was 3.4 MPa and heated to T = 673 K (400 °C), heating rate 100 K/h, hold for 48 h, then cooled to 373 K (100 °C) in 3:30 h finally to room temperature.

2.4. In Situ X-ray Powder Diffraction (XRPD)

A Rigaku SmartLab diffractometer with CuKA1 radiation was used to collect laboratory XRPD data. Cu-K radiation was used to collect in situ X-ray diffraction data on a SmartLab (Rigaku Corporation, Tokyo, Japan) high-resolution X-ray diffractometer with a HyPix-3000 two-dimensional semiconductor detector. Cu-K has been removed from the Cu-K measurements using a nickel filter. Bragg–Brentano geometry was used to operate the diffractometer. Individual measurements took 10 min to collect data and 6 min to collect data for the second $CaNi_2$ measurement. Grinding the reactants and placing it in the sample holder of an Anton Paar (Graz, Austria) XRK 900 Reactor Chamber resulted in flat samples. The chamber's gas supply system was connected, allowing for evacuation and subsequent H_2 gas flooding (H2: Air Liquide, 99.9%). To refine crystal structures, the program FullProf (5.0.0.0) was used [37].

2.5. Characterization

X-ray diffraction (XRD) measurements were performed using a Huber G670 diffractometer with Mo-Kα1 radiation (Provided by Huber Diffraktionstechnik GmbH & Co. KG, Rimsting, Germany) over a 2 θ range of 5–70°. The surface morphology was performed using an Oxford Instruments EDX INCA SYSTEM mounted on a Zeiss LEO 1530 scanning electron microscope with a working distance of 15 mm and an energy dispersive spectrometer (EDS) provided by Oxford company, Scotts Valley, CA, USA. A JEOL 2100 Plus instrument was used for the high-resolution transmission electron microscopy investigations with a point resolution of 0.19 nm.

3. Results

The Rietveld method was used for the evaluation of powder diffraction data, using the FULLPROF software (version: 5.0.0.0). Consecutively, crystal structure refinements were completed. From the Inorganic Crystal structure database (ICSD), the initial's structure was taken. Pseudo-Voigt were used for all refinement in model reflection profiles. Asymmetry, cell parameter, scale factor and Caglioti parameters were refined but the occupation numbers, thermal displacement and atomic position were fixed for all refinements.

Intermetallic samples were grey powders changing to black and becoming more brittle after hydrogenation. Rietveld refinements based on XRPD data were performed using the structure types of $MgNi_2$ type and $MgCu_2$ type as starting models. These structure types could be confirmed by the good fit of the Rietveld refinements (Figure 2a,b). Solid-solutions of $Ca_xMg_{1-x}Ni_2$ crystallize in the hexagonal Laves phase type ($MgNi_2$, C36) for $x \leq 0.33$ and in the cubic Laves phase type ($MgCu_2$, C15) for $0.33 < x$. The refined lattice parameter i.e., structure type and space group type before hydrogenation are given in (Table 1).

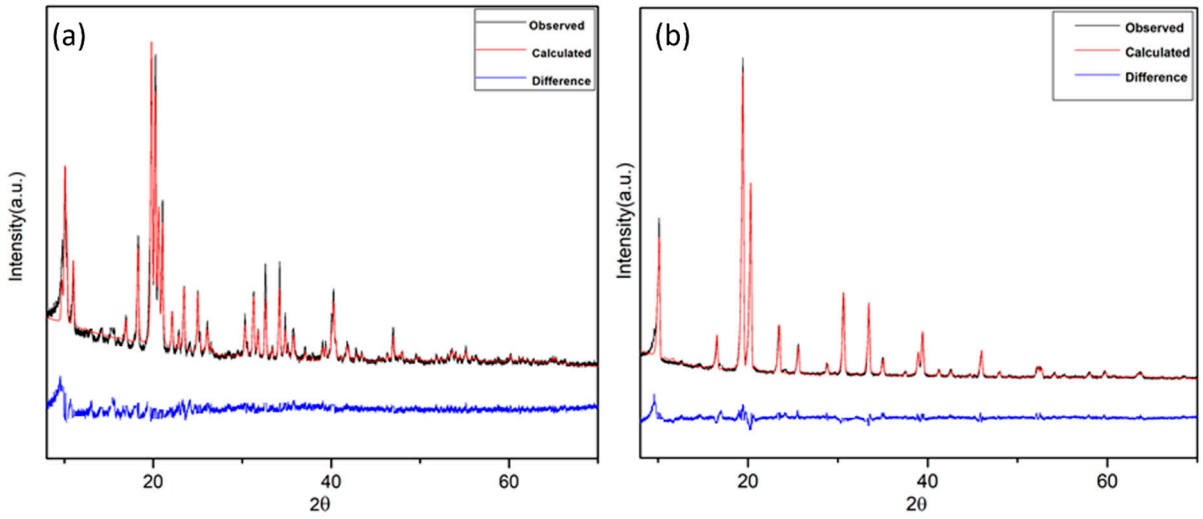

Figure 2. (**a**) Rietveld refinement of the crystal structure of $Ca_xMg_{1-x}Ni_2$ (x = 0.33) in the hexagonal $MgNi_2$ type $P6_3/mmc$, a = 482.585(27) pm, c = 1583.073(106) pm, R_{wp} = 3.76%, χ^2 = 1.85; (**b**) Rietveld refinement of the crystal structure of $Ca_xMg_{1-x}Ni_2$ (x = 0.5) in the cubic $CaNi_2$ type $Fd\bar{3}m$, a = 697.116(32) pm, R_{wp} = 3.11%, χ^2 = 1.34 based on X-ray powder diffraction at 297(1) K ($Mo_{K\alpha1}$ radiation, λ = 70.926 pm).

Table 1. Refined lattice parameters of $Ca_xMg_{1-x}Ni_2$ compounds based on X-ray powder diffraction at 297(1) K.

X	Structure Type	Space Group Type	*a*/pm	*c*/pm
0	$MgNi_2$	$P6_3/mmc$	a = 482.513(68)	c = 1582.073(271)
0.33	$MgNi_2$	$P6_3/mmc$	a = 482.585(27)	c = 1583.073(106)
0.5	$MgCu_2$	$Fd\bar{3}m$	a = 697.116(32)	*A*
0.67	$MgCu_2$	$Fd\bar{3}m$	a = 705.112(24)	*A*
1	$MgCu_2$	$Fd\bar{3}m$	a = 724.063(54)	*A*

After hydrogenation in an autoclave the X-ray diffraction patterns changed completely (Figure 3a,b). Reflections could be assigned to CsCl type cubic structure $CaNiH_3$ and Ni; Rietveld refinement confirmed this. Most Laves phases retained after incorporation of hydrogen their crystal structure except tetrahedral interstices filled by hydrogen atoms and expanded in volume. A suitable hydrogen position is A_2M_2 in cubic Laves phases (C15 type, $Fd\bar{3}m$), tetrahedral interstices on probable Wyckoff position 96 g. In $Ca_xMg_{1-x}Ni_2$ (x = 0.67) the peaks present at the Bragg position (2θ°) 16.240, 23.040, 25.800, 28.320, 32.800, 34.860, 36.820, 42.200, 43.880 and corresponds to the reflection from (110), (200), (210), (211), (220), (300), (310), (320), (321) crystal plane assigned to the cubic perovskite type $CaNiH_3$ and the peaks present at the 2θ° of 20.020, and 40.680 are assigned to Ni. While in the case of $Ca_xMg_{1-x}Ni_2$ (x = 1) the peaks present at the 2θ° 16.237, 25.855, 28.400, 36.888, 44.054, 50.270, 61.409 and 62.704 are assigned to $CaNiH_3$ and the peaks present at the 2θ° 20.020, 23.160, 32.980, 38.770, 40.680, 51.880, 53.340, 58.900 are assigned to the Ni. $MgNi_2$ type structures (C36) such as $Ca_xMg_{1-x}Ni_2$ when $x \leq 0$ absorbed hydrogen at high hydrogen pressure not at low hydrogen pressure confirmed from hydrogenation in autoclave (Figure 3c) and exhibited in hexagonal type crystal structure. The refined lattice parameter i.e., structure type and space group type after hydrogenation are given in (Table 2).

In situ X-ray powder diffraction data were recorded under hydrogen pressure for three different samples (Figures 4–6) i.e., $CaNi_2$, $Ca_{0.5}Mg_{0.5}Ni_2$ and $Ca_{0.67}Mg_{0.33}Ni_2$. Under 0.3 MPa hydrogen pressure the reaction $2CaNi_2 + 3H_2 \rightarrow 2CaNiH_3 + 2Ni$ was followed by in situ X-ray powder diffraction (Figure 4). The reaction temperature was started from 25 to 500 °C completed in 20 °C steps with a 30 °C·min^{-1} ramp. The hydrogen pressure recorded after each 25 °C absorbed by the sample till the temperature reached 500 °C. The temperature holds for 1 h at 500 °C and then cold to room temperature. The $CaNi_2$ has a cubic structure and form the cubic CsCl type hydride. There was no intermediate formed during the above reaction. The same reaction conditions were followed for the cubic $MgCu_2$ type structure $Ca_{0.5}Mg_{0.5}Ni_2 + H_2 \rightarrow Ca_{0.5}Mg_{0.5}Ni_2H_{2.55}$ (Figure 5) and $Ca_{0.67}Mg_{0.33}Ni_2 + H_2 \rightarrow Ca_{0.67}Mg_{0.33}Ni_2H_{2.70}$ (Figure 6).

Before the hydrogenation the refined lattice parameters of the three samples Figures 4–6 are: a = 724.063(54), a = 697.116(32) and a = 705.112(24), respectively. After hydrogenation of the three samples $CaNi_2$, $Ca_{0.5}Mg_{0.5}Ni_2$ and $Ca_{0.67}Mg_{0.33}Ni_2$ (4–6), respectively, by in situ X-ray diffraction the lattice parameters of the hydrogenated sample increased, which is confirmed by the Rietveld refinements of its X-ray diffraction profiles. The refined lattice parameters of the (Figures 4–6) are a = 724.263(54), a = 697.416(32) and a = 705.512(24), respectively, which confirmed the hydrogen absorption by the synthesized compounds.

Mostly materials are the $MgCu_2$ (C15) type structure at the composition when x = 0.5, x = 0.67, x = 1 in the $Ca_xMg_{1-x}Ni_2$ while the materials are the $MgNi_2$ (C36) type structure at the composition when x = 0, x = 33. The synthesized compounds $CaNi_2$, $Ca_{0.5}Mg_{0.5}Ni_2$, $Ca_{0.67}Mg_{0.33}Ni_2$, have cubic crystal structure and the $Ca_{0.33}Mg_{0.67}Ni_2$, $MgNi_2$ have hexagonal crystal structure. It was found from Figures 5 and 6 that x could be increased for $Ca_{0.5}Mg_{0.5}Ni_2$, $Ca_{0.67}Mg_{0.33}Ni_2$, from 2.55 to 2.70. The above materials at 0.1 MPa desorb partially to about x = 1.3. It was concluded that $Ca_{0.5}Mg_{0.5}Ni_2H_{2.6}$, $Ca_{0.67}Mg_{0.33}Ni_2H_{2.6}$ roughly corresponds to 1.7% H_2, and that is why these hydrides may be of interest for technological applications.

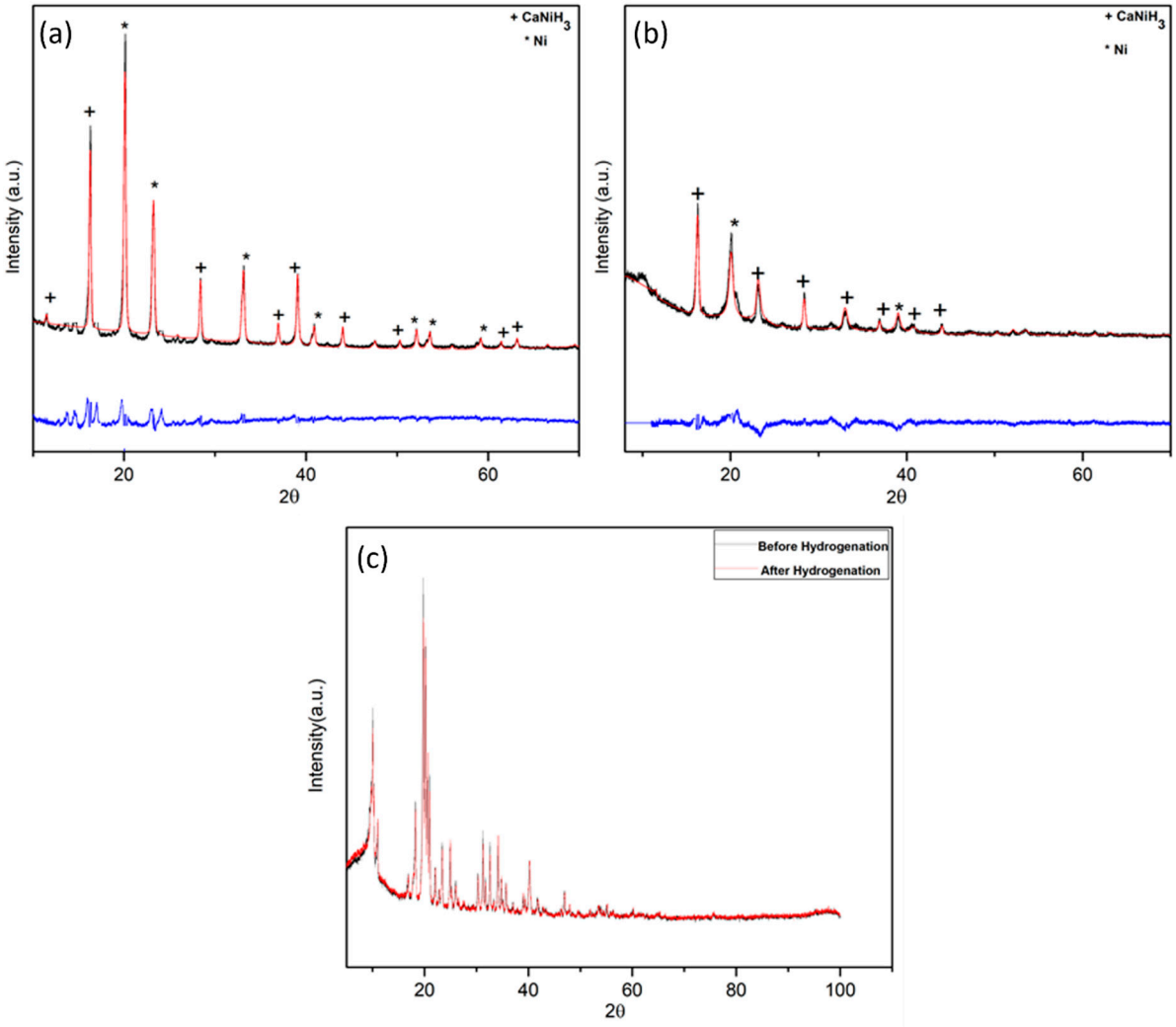

Figure 3. Rietveld refinement of (**a**) $Ca_xMg_{1-x}Ni_2$ (x = 1) R_{wp} = 3.36%, χ^2 = 1.50, (**b**) $Ca_xMg_{1-x}Ni_2$ (x = 0.67) R_{wp} = 2.46%, χ^2 = 1.05, (**c**) $Ca_xMg_{1-x}Ni_2$ (x = 0) R_{wp} = 4.70%, χ^2 = 1.60 after hydrogenation in autoclave based on X-ray powder diffraction at 297(1) K ($Mo_{K\alpha1}$ radiation, λ = 70.926 pm: (Black = observed; Red = calculated and Blue = Difference)).

Table 2. Refined lattice parameters of $Ca_xMg_{1-x}Ni_2$ (x = 1, x = 0.67 and x = 0) compounds after hydrogenation based on X-ray powder diffraction at 297(1) K.

X	Structure Type	Space Group Type	*a*/pm	*c*/pm
0	$MgNi_2$	$P6_3/mmc$	a = 482.637(29)	c = 1583.699(127)
0.67	$MgCu_2$	$Fd\bar{3}m$	a = 705.515(48)	*A*
1	$MgCu_2$	$Fd\bar{3}m$	a = 705.393(21)	*A*

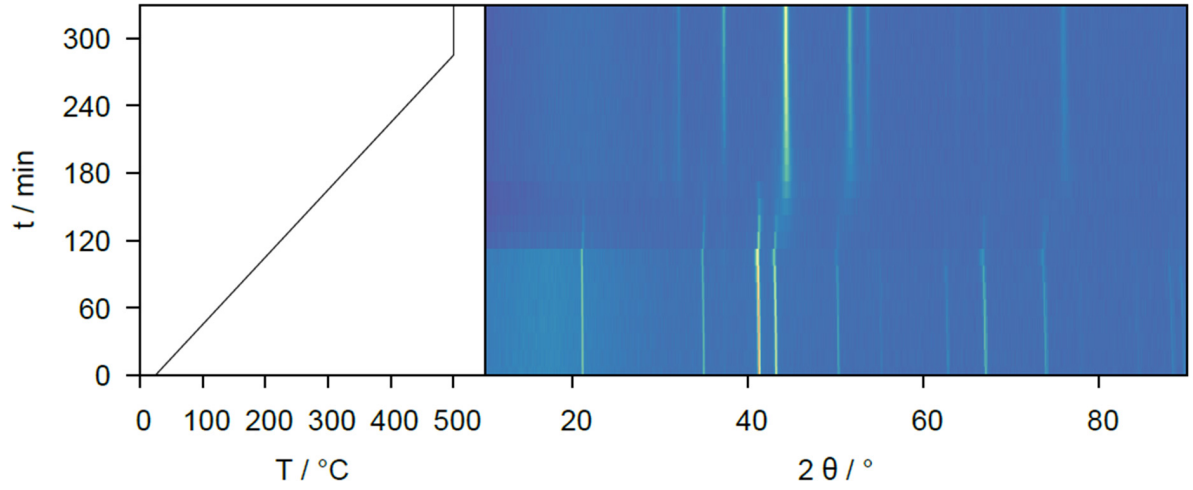

Figure 4. In situ X-ray powder diffraction of $CaNi_2$.

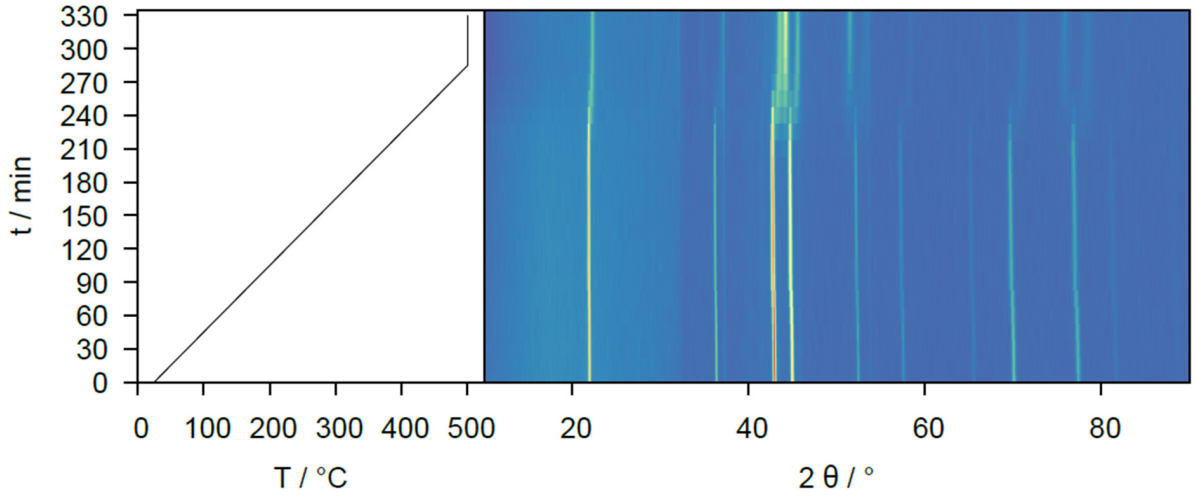

Figure 5. In situ X-ray powder diffraction of $Ca_xMg_{1-x}Ni_2$ (x = 0.5).

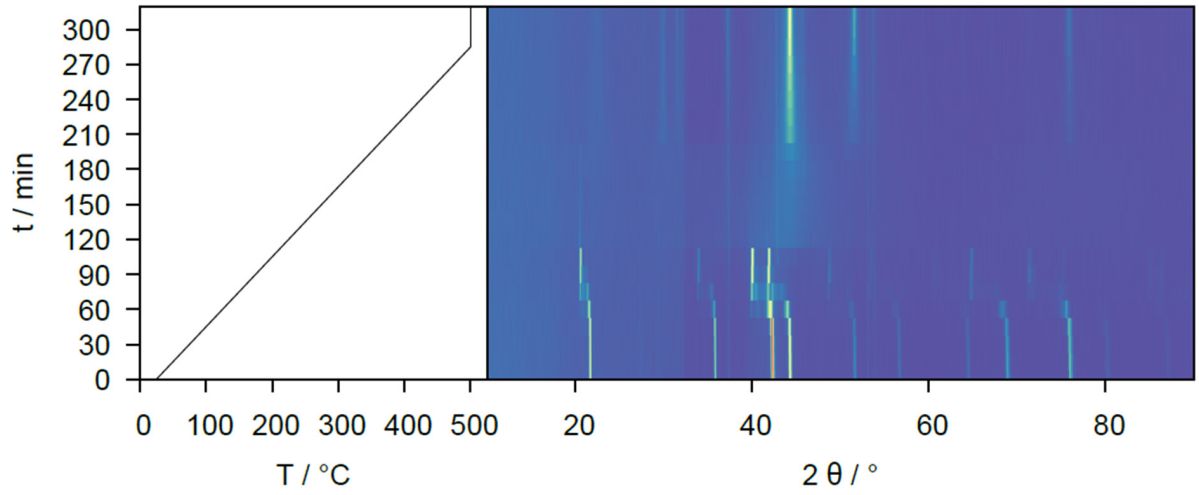

Figure 6. In situ X-ray powder diffraction of $Ca_xMg_{1-x}Ni_2$ (x = 0.67) under 0.3 MPa hydrogen gas flow (15 sccm), data collected on a Rigaku SmartLab diffractometer in an Anton Paar XRK 900 Reactor Chamber using Cu-Kα1 radiation, sample heated in 20 K steps for 25 °C $\leq$ T $\leq$ 500 °C with a 30 K·min^{-1} ramp.

According to the Orimo at al., amorphous MgNi and its hydrides have local structure related to CsCl type structures [37,38]. It is known that Mg is an alkaline-earth element as well as Ca, so it is possible that Mg and Ca have some crystallographic structural similarities. The present result obtained from the Rietveld refinement supports their results for the MgNi hydride. However, there are some differences between the CaNi and MgNi hydrogenation properties. The MgNi has hydrogen content 1 H/M and CaNi has hydrogen content 1.5 H/M which is more than MgNi [39,40]. The MgNi shows a reversible hydrogenation and dehydrogenation while CaNi does not show the reversibility with hydrogen gas for the reaction.

The SEM analysis was carried out to for morphological examination and homogenized nature of the prepared derivation of $Ca_xMg_{1-x}Ni_2$ ($0 \leq x \leq 1$) as shown Figure 7a–d. The micrographs reveal the formation of larger particles due to the aggregation of small particles. The large size aggregates are unevenly distributed and, due to the irregular shape and size, it is difficult to identify the exact morphology and particles size from the SEM micrographs.

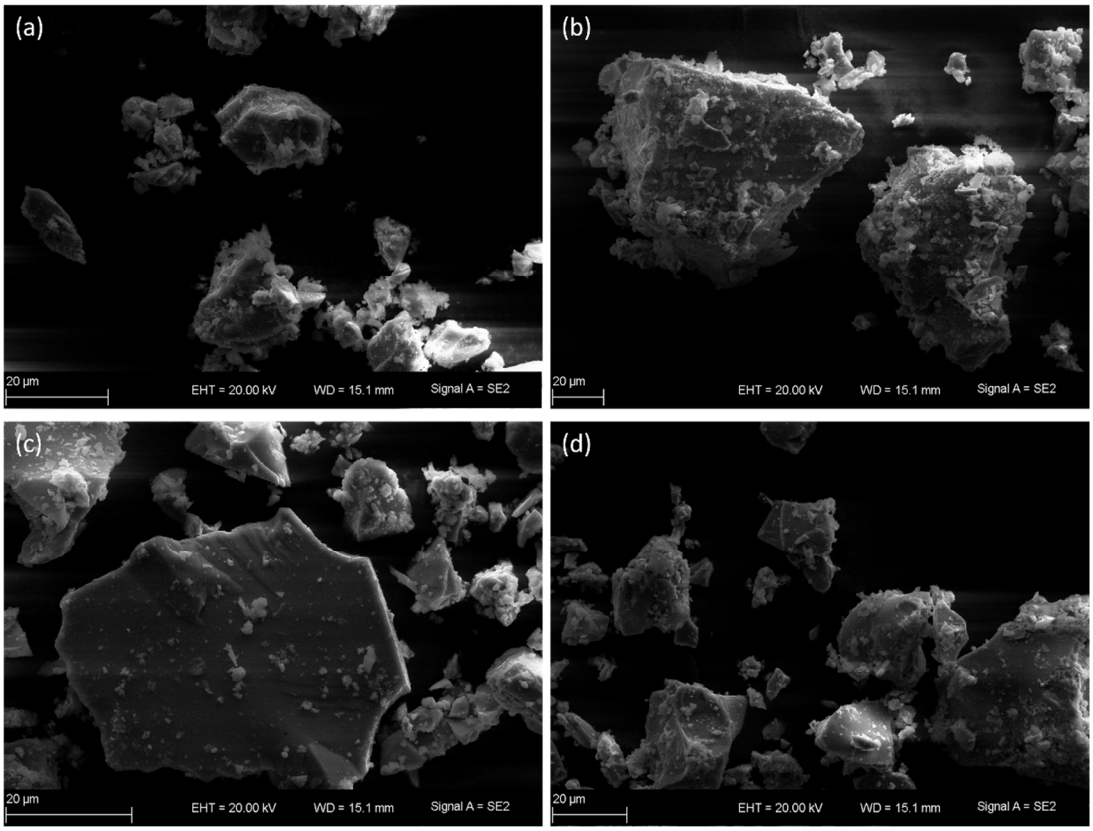

Figure 7. SEM micrograph of (**a**) $MgNi_2$, (**b**) $Ca_xMg_{1-x}Ni_2$ ($x = 0.33$), (**c**) $CaNi_2$, (**d**) $Ca_xMg_{1-x}Ni_2$ ($x = 0.5$).

The elemental composition and percentage purity of the synthesized derivatives of $Ca_xMg_{1-x}Ni_2$ ($0 \leq x \leq 1$) were evaluated through EDX analysis. EDX elemental mapping shows the uniform distribution of Ca, Ni and Mg in their respective samples as shown in Figure 8a–d. The EDS spectrum for $CaNi_2$, (Figure 8b) exhibits the sharp signals at 0.35, 3.7, 4.0 keV for Ca and 0.7, 7.5 and 8.25 keV for Ni, where the weight percent of 24.96 and 75.05 were reported for Ca and Ni, respectively. The composition of $Ca_{0.5}Mg_{1-0.5}Ni_2$ is evident from the EDS spectrum given in Figure 8b, where Ca, Mg and Ni are present in the sample with weight percent of 15.51, 10.69 and 73.80, respectively. The composition of $Ca_{0.33}Mg_{0.67}Ni_2$ has been confirmed from the EDS spectrum shown in Figure 8c. The weight percent of the Ca, Mg and Ni are 9.48, 3.23 and 87.29 determined during elemental analysis. The Figure 8d reveals the composition of $MgNi_2$, the peaks for the Ni were observed at

0.85, 7.5 and 8.35 keV and present Mg in the sample was confirmed by the peak at 1.25 keV. The weight percent for Ni and Mg was found to be 64, 83 and 35.17, respectively.

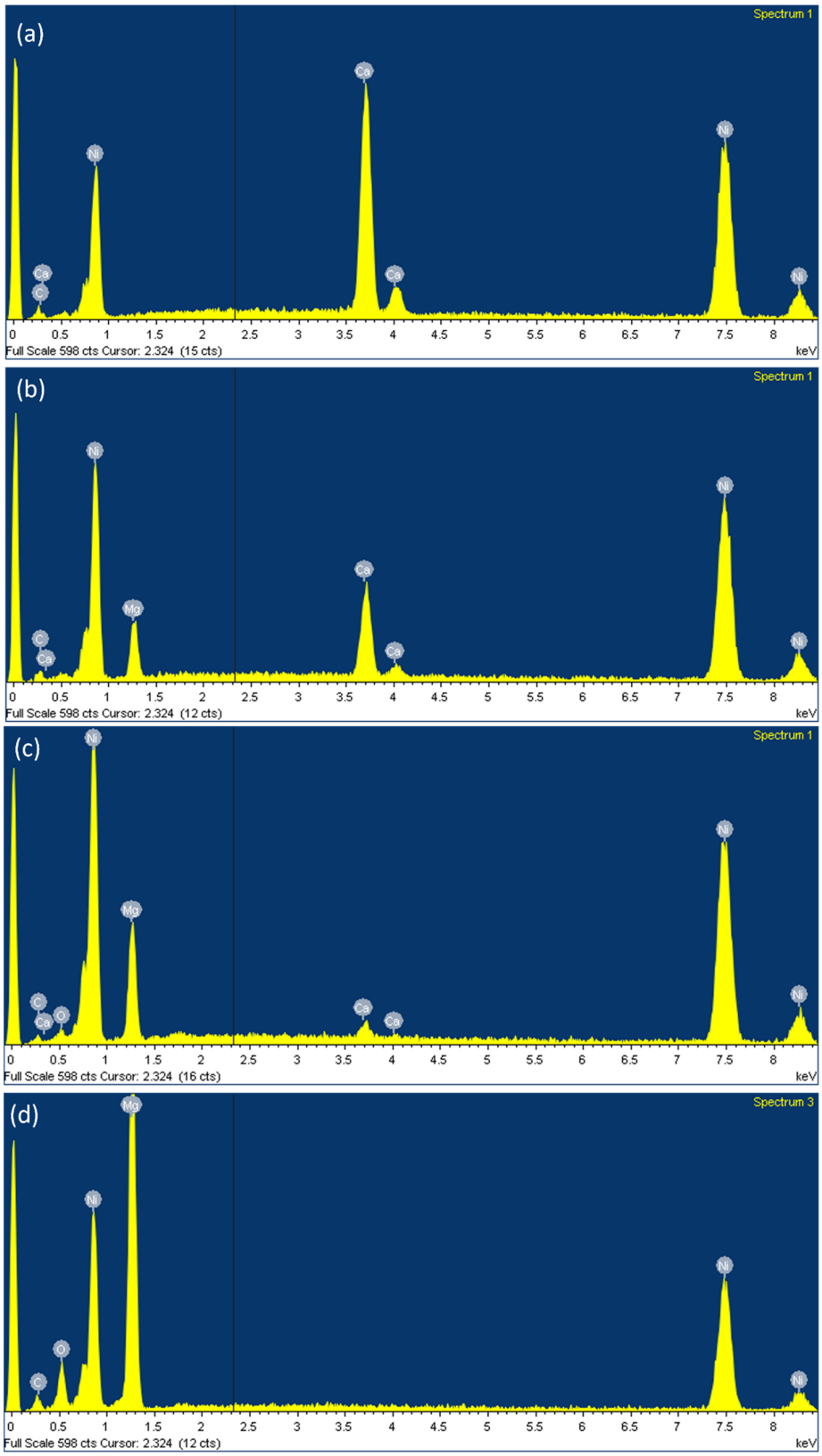

Figure 8. EDS spectra of the (**a**) $CaNi_2$ (**b**) $Ca_xMg_{1-x}Ni_2$ (x = 0.5) (**c**) $Ca_xMg_{1-x}Ni_2$ (x = 0.33) (**d**) $MgNi_2$.

To confirm the above XRD results HRTEM were performed for the $CaNi_2$ and $Ca_xMg_{1-x}Ni_2$ (x = 0.5). Figure 9a–d show the TEM images of $CaNi_2$ and $Ca_xMg_{1-x}Ni_2$ (x = 0.5). From the TEM images it was confirmed that the synthesized compounds are crystalline. Crystallographic information and d-spacing of the crystal planes were determined by selected area electron diffraction. Figure 10a showed the SAED of $CaNi_2$ and Figure 10b, c of $Ca_xMg_{1-x}Ni_2$ (x = 0.5). Selected area electron diffraction patterns along the different directions of $CaNi_2$ and $Ca_xMg_{1-x}Ni_2$ (x = 0.5) were taken. Figure 10 showed that for these images of single crystal, it is simply dots, and that these dots are located at the same position with regard one another. Thus, there is a complete order. Figure 10 showed that the diffraction gives discrete parts because in a single crystal all atoms are in the same order to all the edges of materials. The surface morphology of the synthesized materials was rough and porous, which is suitable for hydrogen storage.

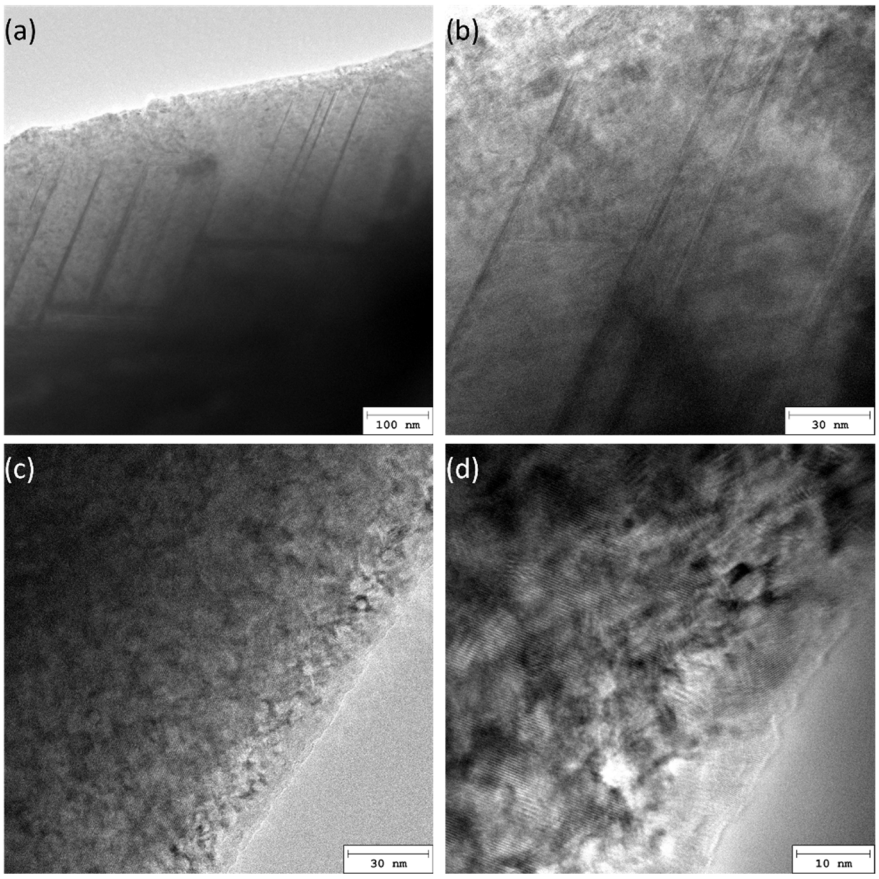

Figure 9. HTEM images of (**a**,**b**) $CaNi_2$ (**c**,**d**) $Ca_xMg_{1-x}Ni_2$ (x = 0.5) at high magnification.

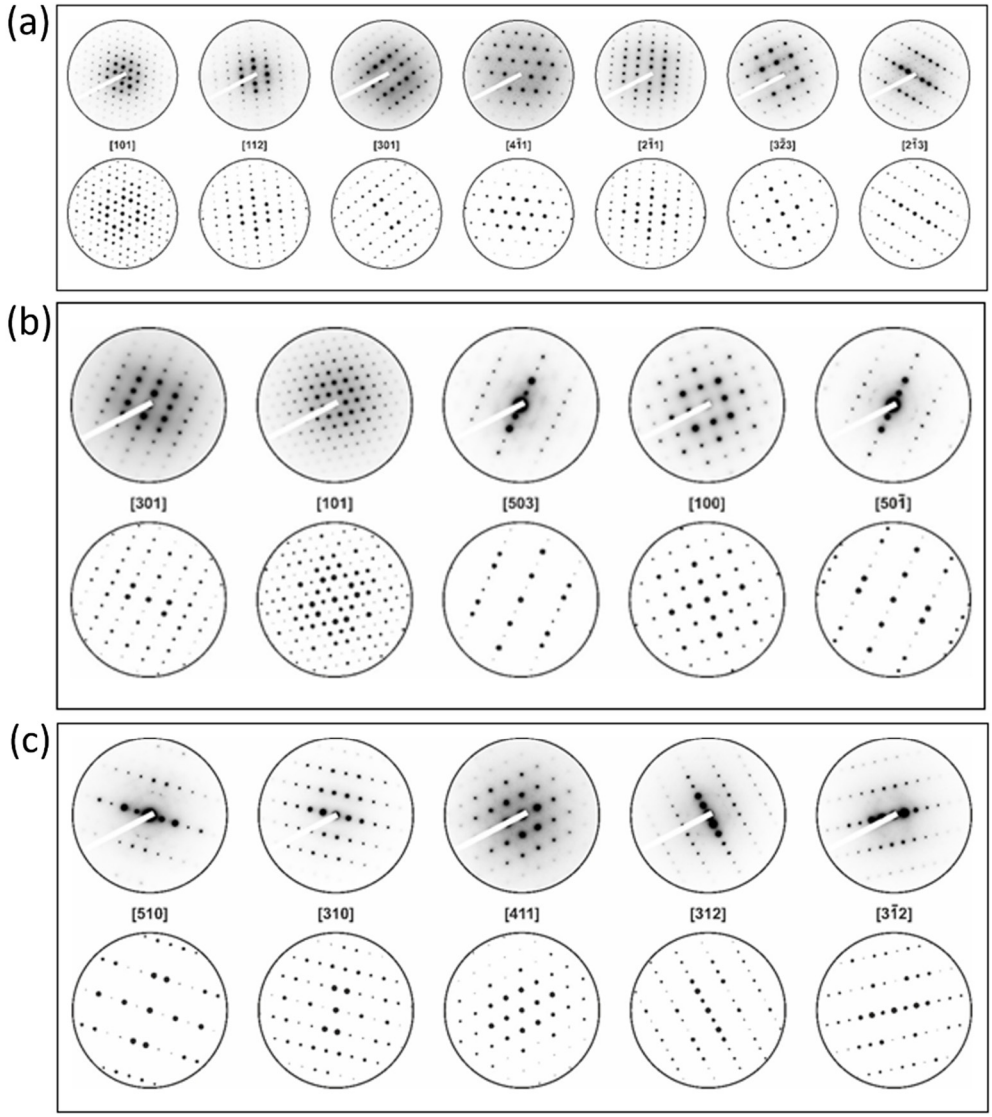

Figure 10. SAED analysis of (**a**) $CaNi_2$ (**b**,**c**) $Ca_xMg_{1-x}Ni_2$ (x = 0.5).

4. Conclusions

For technological applications the hydriding behavior of these materials make them interesting as potential hydrogen storage with tailored properties to exploit the adverse kinetic effects upon Mg incorporation for hindering decomposition. After hydrogenation, there is in autoclave growth of crystallites of CaNi hydride and Ni. Elemental hydride absorbed hydrogen (CaH_2 + $NiH_{0.7}$ = $CaNiH_{2.7}$) so that the hydrogen absorbed by the synthesized $CaNiH_3$ in autoclave is approximately equal. Laves phases based on $MgCu_2$ (C15) and $MgNi_2$ (C36) retained their crystal structures upon hydrogenation. The $MgNi_2$ type structures (C36) such as $Ca_xMg_{1-x}Ni_2$ absorbed hydrogen at high hydrogen pressure when $x \leq 0$, not at low hydrogen pressure, which was concluded from hydrogenation in autoclave and exhibited in the hexagonal type crystal structure. The $MgCu_2$ type structures (C15) such as $Ca_xMg_{1-x}Ni_2$ when $x \leq 1$ absorbed hydrogen at a low pressure, confirmed by in situ X-ray diffraction and in the autoclave hydrogenation study, and as exhibited in cubic crystal structure.

Author Contributions: Conceptualization, Z.U.R., M.N. and H.U.; methodology, H.U.; software, S.H.; validation, P.A. and M.U.K.; formal analysis, Z.U.R.; investigation, H.U.; resources, H.U.; data curation, P.A.; writing—original draft preparation, Z.U.R.; writing—review and editing, S.H., A.M.I.

and A.S.; visualization, H.U.; supervision, M.N.; project administration, M.N.; funding acquisition, A.M.I. and A.S. All authors have read and agreed to the published version of the manuscript.

Funding: This research was funded by Deanship of Scientific Research at King Khalid University for funding this work through Group Research Project under grant number (R.G.P.2/33/42).

Institutional Review Board Statement: Not applicable.

Informed Consent Statement: Not applicable.

Data Availability Statement: All the data is available within the manuscript.

Acknowledgments: The authors extend their appreciation to the Deanship of Scientific Research at King Khalid University for funding this work through Group Research Project under grant number (R.G.P.2/33/42). One of the authors (Zia Ur Rehman) is highly thankful to HEC (Higher Education Commission of Pa-kistan) for its financial support provided through NRPU research grant and IRSIP (International Research Support Initiative Program) for carrying out part of the research work at Institute of Inor-ganic Chemistry, Leipzig University, Germany under the guidance of Holger Kohlmann for which the gratitude is extended to him as well.

Conflicts of Interest: The authors declare no conflict of interest.

References

1. Vajeeston, P.; Ravindran, P.; Fjellvåg, H. Predicting New Materials for Hydrogen Storage Application. *Materials* **2009**, *2*, 2296–2318. [CrossRef]
2. Zhu, M.; Lu, Y.; Ouyang, L.; Wang, H. Thermodynamic Tuning of Mg-Based Hydrogen Storage Alloys: A Review. *Materials* **2013**, *6*, 4654–4674. [CrossRef] [PubMed]
3. Rivard, E.; Trudeau, M.; Zaghib, K. Hydrogen Storage for Mobility: A Review. *Materials* **2019**, *12*, 1973. [CrossRef]
4. Li, H.W.; Yan, Y.; Orimo, S.I.; Züttel, A.; Jensen, C.M. Recent Progress in Metal Borohydrides for Hydrogen Storage. *Energies* **2011**, *4*, 185–214. [CrossRef]
5. Møller, K.; Sheppard, D.; Ravnsbæk, D.; Buckley, C.; Akiba, E.; Li, H.W.; Jensen, T. Complex Metal Hydrides for Hydrogen, Thermal and Electrochemical Energy Storage. *Energies* **2017**, *10*, 1645. [CrossRef]
6. Xueping, Z.; Jiaojiao, Z.; Shenglin, L.; Xuanhui, Q.; Ping, L.; Yanbei, G.; Weihua, L. A new solid material for hydrogen storage. *Int. J. Hydrogen Energy* **2015**, *40*, 10502–10507. [CrossRef]
7. Hardy, B.; Tamburello, D.; Corgnal, C. Hydrogen storage adsorbent systems acceptability Envelope. *Int. J. Hydrogen Energy* **2018**, *43*, 19528–19539. [CrossRef]
8. Gao, S.; Liu, H.; Xu, L.; Li, S.; Wang, X.; Yan, M. Hydrogen storage properties of nano-CoB/CNTs catalysed MgH2. *J. Alloys Compd.* **2018**, *735*, 635–642. [CrossRef]
9. Momirlan, M.; Veziroglu, T.N. Current status of hydrogen energy. *Renew. Sustain. Energy Rev.* **2002**, *6*, 141–179. [CrossRef]
10. Cabo, M.S.; Garroni, S.; Pellicer, E.; Milanese, C.; Girella, A.; Marini, A.; Rossinyol, E.; Suriñach, S.; Baro, M.D. Hydrogen sorption performance of MgH2 doped with mesoporous nickel- and cobalt-based oxides. *Int. J. Hydrogen Energy* **2011**, *36*, 5400–5410. [CrossRef]
11. Charbonnier, J.; de Rangoa, P.; Fruchart, D.; Miragliaa, S.; Pontonnier, L.; Rivoirard, S.; Skryabina, N.; Vulliet, P. Hydrogenation of transition element additives (Ti, V) during ball milling of magnesium hydride. *J. Alloys Compd.* **2004**, *383*, 205–208. [CrossRef]
12. Li, Y.; Hu, F.; Luo, L.; Xu, J.; Zhao, Z.; Zhang, Y.; Zhao, D. Hydrogen storage of casting MgTiNi alloys. *Catal. Today* **2018**, *318*, 103–106. [CrossRef]
13. Witek, K.; Karczewski, K.; Karpowicz, M.; Polanski, M. Mg_2FeH_6 Synthesis Efficiency Map. *Crystals* **2018**, *8*, 94. [CrossRef]
14. Varin, R.A.; Czujko, T.; Wronski, Z.S. Thermal stability of Vale Inco nanonometric nickel as a catalytic additive for magnesium hydride (MgH2). *Int. J. Hydrogen Energy* **2009**, *34*, 8603–8610. [CrossRef]
15. Sandrock, G.D.; Murrary, J.J.; Post, M.; Taylor, L. Hydrides and deuterides of $CaNi_5$. *Mater. Res. Bull.* **1982**, *17*, 887–894. [CrossRef]
16. Kadir, K.; Kuriyama, N.; Sakai, T.; Uehara, I.; Eriksson, L. Structural investigation and hydrogen capacity of $CaMg_2Ni_9$: A new phase in the AB_2C_9 system isostructural with $LaMg_2Ni_9$. *J. Alloys Compd.* **1999**, *284*, 145–154. [CrossRef]
17. Kadir, K.; Sakai, T.; Uehara, I. Structural investigation and hydrogen capacity of YMg_2Ni_9 and $(Y_{0.5}Ca_{0.5})$ (MgCa)Ni_9: New phases in the AB_2C_9 system isostructural with $LaMg_2Ni_9$. *J. Alloys Compd.* **1999**, *287*, 264–270. [CrossRef]
18. Liang, G.; Schulz, R. Phase structures and hydrogen storage properties of Ca–Mg–Ni alloys prepared by mechanical alloying. *J. Alloys Compd.* **2003**, *356/357*, 612. [CrossRef]
19. Laves, F.; Wallbaum, H.J. Über den Einfluß geometrischer Faktoren auf die stöchiometrische Formel metallischer Verbindungen, gezeigt an der Kristallstruktur des KNa2. *Z. Anorg. Allg. Chem.* **1942**, *250*, 110–120. [CrossRef]
20. Laves, F. *Factors Governing Crystal Structure in Intermetallic Compounds*; Westbrook, J.H., Ed.; John Wiley & Sons: New York, NY, USA, 1967; pp. 129–143.
21. Nesper, R. Chemische bindungen—Intermetallische verbindungen. *Angew. Chem.* **1991**, *7*, 805–834. [CrossRef]

22. Shaltiel, D.; Jacob, I.; Davidov, D. Hydrogen absorption and desorption properties of AB2 Laves-Phase pseudobinary compounds. *J. Less-Common Met.* **1977**, *53*, 117–131. [CrossRef]
23. Shaltiel, D. Hydride properties of AB2 Laves Phase compounds. *J. Less-Common Met.* **1978**, *62*, 407–416. [CrossRef]
24. Shoemaker, D.P.; Shoemaker, C.B. Concerning atomic sites and capacities for hydrogen absorption in the AB2 Friauf-Laves Phases. *J. Less-Common Met.* **1979**, *68*, 43–58. [CrossRef]
25. Ivey, D.G.; Northwood, D.O. Storing Hydrogen in AB2 Laves-type compounds. *Z. Phys. Chem.* **1986**, *147*, 191–209. [CrossRef]
26. Miedema, A.R.; Buschow, K.H.J.; Van Mal, H.H. Which intermetallic compounds of transition metals form stable hydrides? *J. Less-Common Met.* **1976**, *49*, 463–472. [CrossRef]
27. Oesterreicher, H.; Ensslen, K.; Kerlin, A.; Bucher, E. Hydriding Behavior in Ca-Mg-Ni-B. *Mater. Res. Bull.* **1980**, *15*, 275–283. [CrossRef]
28. Terashita, N.; Kobayashi, K.; Sakai, T.; Akiba, E. Structural and hydriding properties of $(Mg_{1-x}Ca_x)Ni_2$ Laves phase alloys. *J. Alloys Compd.* **2001**, *327*, 275–280. [CrossRef]
29. Kadir, K.; Uehara, I.; Sakai, T. Synthesis and structure determination of a new series of hydrogen storage alloys; RMg2Ni9 (R = La, Ce, Pr, Nd, Sm and Gd) built from $MgNi_2$ Laves-type layers alternating with AB_5 layers. *J. Alloys Compd.* **1997**, *257*, 115–121. [CrossRef]
30. Orimo, S.; Fujii, H. Effects of nanometer-scale structure on hydriding properties of Mg-Ni alloys: A review. *Intermetallics* **1998**, *6*, 185. [CrossRef]
31. Orimo, S.; Fujii, H. Materials science of Mg-Ni-based new hydrides. *Appl. Phys. A* **2001**, *72*, 167. [CrossRef]
32. Tsushio, Y.; Akiba, E. Hydrogenation properties of Mg-based Laves phase alloys. *J. Alloys Comp.* **1998**, *269*, 219. [CrossRef]
33. Tsushio, Y.; Tessier, P.; Enoki, H.; Akiba, E. Hydrogenation properties of $Mg_{1-x}M_{1x}Cu_2$ (M1 = La and Nd) with larger interstitial sites than $MgCu_2$. *J. Alloys Comp.* **1998**, *280*, 262. [CrossRef]
34. Oesterreicher, H.; Bittner, H. Hydride formation in $La_{1-x}Mg_xNi_2$. *J. Less-Common Met.* **1980**, *73*, 339. [CrossRef]
35. Kohno, T.; Yoshida, V.; Kawashima, F.; Inaba, T.; Sakai, I.; Yamamoto, M.; Kanda, M. Hydrogen storage properties of new ternary system alloys: La_2MgNi_9, $La_5Mg_2Ni_{23}$, La_3MgNi_{14}. *J. Alloys Comp.* **2000**, *311*, L5–L7. [CrossRef]
36. Miraglia, S.; Girard, G.; Fruchart, D.; Liang, G.; Huot, J.; Schulz, R. Structural characterization and some hydrogen absorption properties of $(Mg_xCa_{1-x})Ni_{2.6}$: A new phase in the Mg–Ca–Ni system. *J. Alloys Compd.* **2009**, *478*, 33–36. [CrossRef]
37. Rodríguez-Carvajal, J. *FullProf: A Program for Rietveld Refinement and Pattern Matching Analysis*; Institute Laue-Langevin: Grenoble, France, 2012.
38. Orimo, S.; Ikeda, K.; Fujii, H.; Saruki, S.; Fukunaga, T.; Zu¨ttel, A.; Schlapbach, L. Hydriding properties of the MgNi-based systems. *J. Alloys Comp.* **1998**, *293*, 437–442. [CrossRef]
39. Orimo, S.; Ikeda, K.; Fujii, H.; Saruki, S.; Fukunaga, T. Hydriding properties of the MgNi-H (D) system with amorphous single phase-Investigation from a viewpoint of the short range ordering. *Nippon Kinzoku Gakkaishi/J. Jpn. Inst. Met.* **1999**, *63*, 959–964. [CrossRef]
40. Orimo, S.; Fujii, H.; Ikeda, K.; Fujikawa, Y.; Kitano, Y. Hydriding properties of a nano-/amorphous-structured Mg–Ni–H system. *J. Alloys Comp.* **1997**, *94*, 253–254. [CrossRef]